

Break Point Detection for Functional Covariance

Shuhao Jiao^{*1}, Ron D. Frostig^{†2}, and Hernando Ombao^{‡1}

¹Statistics Program, KAUST, Saudi Arabia

²Department of Neurobiology and Behavior, UC Irvine, USA

Abstract

Many experiments record sequential trajectories that oscillate around zero. Such trajectories can be viewed as zero-mean functional data. When there are structural breaks (on the sequence of curves) in higher order moments, it is often difficult to spot these by mere visual inspection. Thus, we propose a detection and testing procedure to find the change-points in functional covariance. The method is fully functional in the sense that no dimension reduction is needed. We establish the asymptotic properties of the estimated change-point. The effectiveness of the proposed method is numerically validated in the simulation studies and an application to study structural changes in rat brain signals in a stroke experiment.

Key words: Change-point analysis; Functional covariance structure; Functional data analysis; Functional time series; Local field potentials.

1 Introduction

Functional data analysis has attracted attention of researchers in the last few decades and many methods for structural break detection for functional data have been developed. Here, we propose a novel method of detecting and testing structural breaks in functional covariance. The motivation of this paper comes from a neuroscience experiment conducted by co-author Frostig (see Wann, 2017) to investigate changes in the rat brain following an induced ischemic stroke. Local field potentials (LFP) are recorded from 32 implanted tetrodes on the rat brain cortex during the pre-stroke and post-stroke phase (each phase consisted of five minutes of recording) which are segmented into one-second epochs. Thus we have multivariate (32-dimensional) functional curves for each epoch and a total of 300 epochs for the pre-stroke phase and also 300

^{*}shuhao.jiao@kaust.edu.sa

[†]rfrostig@uci.edu

[‡]hernando.ombao@kaust.edu.sa

for the post-stroke phase. We expect structural change in each LFP tetrode following a stroke. Note, however, that one should not assume the structural change to take place immediately upon the clamping of the artery (simulating ischemic stroke) because there may be some time delay or lag till changes in the brain signals are manifested. Here, all trajectories have constant mean and thus fluctuate around 0 for both pre-stroke and post-stroke and thus our goal here is to develop a method for detecting a change-point method in the functional covariance. To the best of our knowledge, this is the first paper on change-point detection for functional covariance.

Existing work on functional structural break analysis mainly focus on mean function. As an example, consider a series of random functions $\{Y_i(t) : i \in \mathbb{N}\}$ recorded sequentially, the task is to detect the change-point in the sequence, denoted k^* . Berkes et al. (2009) proposed to test the null hypothesis by checking the structural break of functional principal components, and Aue et al. (2009a) quantified the large sample behavior of the change-point estimator. Aston et al. (2012a) extended their results to dependent functional data. Torgovitski (2015) proposed change-aligned principal components for such change-point problems. Aue et al. (2014) proposed a method to check the change-point of coefficient operators in potentially non-homogeneous functional autoregressive model. Aue et al. (2018) proposed a fully functional detecting procedure without any dimension reduction. These methods, however, all focus only on the mean function. This limitation serves as a motivation to develop a change-point detection method for functional covariance.

Meanwhile, there are existing methods related to change-point detection of functional covariance. Aue et al. (2020) dealt with analyzing structural break of spectrum and trace of covariance operator. Aue et al. (2009b) studied the structural break detection problem for the covariance matrix of multivariate time series. They proposed to stack the lower triangular elements of covariance matrix and detect the structure break of the concatenated vectors. One limitation of this method is that it cannot be extended to functional data, since lower triangular elements are not defined for functional covariance. Aston et al. (2012b) and Gromenko et al. (2017) studied the structural break problem for two-way functions, specifically, spatial-temporal data and fMRI data, but they assume separability of the functional covariance of two-way functions. This is essentially rank-1 approximation of the functional covariance, which could be overly restrictive for practical data analysis. Comparing with their work, we study the structural break for the complete functional covariance structure and no separable assumption is made, making it suitable for a broad range of cases.

There are other change-point methods that can be applied to structural break detection in brain signals. Fryzlewicz & Rao (2014) proposed the “BASTA” method for detecting multiple change points in the structure of an auto-regressive conditional heteroscedastic model. Kirch et al. (2015) used VAR model to detect change-points in multivariate time series and applied the method to EEG sequences. Cho & Fryzlewicz (2015) proposed a sparsified binary segmentation method for the second-order structure of a multivariate time series. Schröder & Ombao (2017) proposed a FreSpeD method to detect the change-point in spectrum and coherence sequences of multivariate time

series. Sundararajan & Pourahmadi (2018) proposed a nonparametric method to detect multiple change-points in multivariate time series based on difference in the spectral density matrices. Other works on this topic include Jones et al. (1969), Hively et al. (2000) and Saaïd et al. (2011). As discussed, our method can be used to detect the structural break in brain signals by checking the change point in the functional covariance. Comparing with other works, our procedure focuses on the “big picture” of brain signals. Specifically, we aim to find the change-points in the sequences of functional epochs/trials instead of univariate brain signal recordings. Thus the procedure is more robust to chance variability and random errors, because it is nearly impossible that all observations in an epoch are contaminated by chance variability when there is no pronounced structural breaks, and the chance variability can be attenuated by functional smoothing techniques. Another advantage of our functional procedure lies in the intra-curve information. As the new functional procedure checks the structural break of the entire functional covariance, thus intra-curve information is incorporated, which can potentially reveal the structural break. This is discussed in more details in simulation studies. This paper provides a new perspective for change-point problem of brain signal data.

The major contribution of this article is developing a fully functional procedure to detect the change-point in functional covariance. We consider a general situation where functions can be weakly correlated (see Hörmann et al. (2010)), and the proposed procedure also naturally works for independent functions. Dimension reduction techniques, such as functional principal component analysis, are very popular in functional data analysis. However, they will automatically lead to a loss of information. This loss of information may not be crucial for functional reconstruction but could be critical for change-point detection. Indeed, when the leading principal components are orthogonal to the discrepancy function (here, the difference of functional covariance), it is always better to employ fully functional procedure without dimension reduction regardless of the sample size, because the leading principal components cannot explain the discrepancy at all. Here, we also establish the asymptotic behavior of the estimated change-point.

The rest of the article is organized as follows. In Section 2, we present some preliminaries of functional data, especially the spectral decomposition of two-way functions. In Section 3, we develop the change-point model for functional covariance, along with the estimating, detection and testing procedure. We also derive the asymptotic properties of the proposed change-point estimator. In Section 4, we display some simulation results. Section 5 shows the real data analysis on local field potentials, and Section 6 makes the conclusion. Proof of the theorems in the article can be found in the supplement material.

2 Spectral Decomposition of Two-way Functional Data

We consider a series of continuous random functions $\{Y_i(t) : i \in \mathbb{N}\}$ over $i \in \mathbb{N}$, and each function $Y_i(t)$ is defined over a compact support $t \in \mathcal{T} \subset \mathbb{R}$. We denote the space composed of square integrable functions defined over \mathcal{T} as $L^2(\mathcal{T})$. The mean function of $Y_i(t)$ is assumed to be homogeneous across $i \in \mathbb{N}$ and is defined as follows

$$\mu(t) = E\{Y_i(t)\},$$

which we assume, without loss of generality, to be $\mu(t) = 0$. For the moment, we assume the covariance operator $\Gamma(x)$, which is of major interest in this paper, is also homogeneous across i , and is defined as

$$\Gamma(x)(t) = E\{\langle Y_i, x \rangle Y_i(t)\}, \quad C(t, s) = E\{Y_i(t)Y_i(s)\}.$$

where $C(t, s)$ is the covariance kernel, and the inner product is defined as

$$\langle x, y \rangle = \int x(t)y(t)dt, \quad x, y \in L^2(\mathcal{T}).$$

Notationally, define $X_i(t, s) = Y_i(t)Y_i(s)$, $t, s \in \mathcal{T}$ as the data analogue of the functional covariance, and denote $L^2(\mathcal{T} \times \mathcal{T})$ to be the space of square integrable continuous functions defined over $\mathcal{T} \times \mathcal{T}$. For any $X_i(t, s)$, $X_j(t, s) \in L^2(\mathcal{T} \times \mathcal{T})$, we define the inner product of the two-way functions as

$$\langle\langle X_i, X_j \rangle\rangle = \int_{\mathcal{T} \times \mathcal{T}} X_i(t, s)X_j(t, s)dtds.$$

and norm as

$$\|X_i\|^2 = \int_{\mathcal{T} \times \mathcal{T}} X_i^2(t, s)dtds,$$

where $\|X_i\|^2 < \infty$ for any $i \in \mathbb{N}$.

Similarly, we can define the mean function of $\{X_i(t, s) : i \in \mathbb{N}\}$ as

$$\mu_X(t, s) = E\{X_i(t, s)\} = C(t, s),$$

and covariance operator and auto-covariance operator as

$$\Gamma_{X,h}(x)(t, s) = E\{\langle\langle X_i - C, x \rangle\rangle (X_{i+h}(t, s) - C(t, s))\}, \quad h \in \mathbb{N}, \quad x \in L^2(\mathcal{T} \times \mathcal{T}),$$

with covariance and auto-covariance kernel

$$C_{X,h}(t, s, \tilde{t}, \tilde{s}) = E\{(X_i(t, s) - C(t, s))(X_{i+h}(\tilde{t}, \tilde{s}) - C(\tilde{t}, \tilde{s}))\}, \quad h \in \mathbb{N}.$$

Our procedure involves long-run functional covariance of $\{X_i(t, s) : i \in \mathbb{N}\}$, defined as the summation of all lagged functional covariances presented below

$$LC_X(t, s, \tilde{t}, \tilde{s}) = \sum_{h=-\infty}^{\infty} C_{X,h}(t, s, \tilde{t}, \tilde{s}),$$

and it is evident that LC_X is a positive definite kernel in $L^2(\mathcal{T} \times \mathcal{T})$, and thus admits the following representation by Theorem 1.1 in Ferreira & Menegatto (2009),

$$LC_X(t, s, \tilde{t}, \tilde{s}) = \sum_{d=1}^{\infty} \rho_d \psi_d(t, s) \psi_d(\tilde{t}, \tilde{s}), \quad (2-1)$$

where the two-way eigenfunctions $\{\psi_d(t, s): d \in \mathbb{N}_+\}$ form an series of orthonormal basis of $L^2(\mathcal{T} \times \mathcal{T})$, and the eigenvalues $\{\rho_d: d \in \mathbb{N}_+\}$ account for the variability of the principal components $\{\langle X, \psi_d \rangle: d \in \mathbb{N}_+\}$. Equation (2-1) presents a generalized version of Mercer's theorem.

3 Main results

3.1 Detection and testing procedure

In the case of single change-point, we assume the following change-point model for the functional covariance

$$E\{X_i(t, s)\} = C^{(1)}(t, s)\mathbb{I}(i \leq k^*) + C^{(2)}(t, s)\mathbb{I}(i > k^*), \quad (3-1)$$

and for simplicity, we assume there is no structural break in mean function. The interest here is to test if the functional covariance remains constant across functions i , specifically, we want to test the hypothesis

$$H_0: C^{(1)}(t, s) = C^{(2)}(t, s) = C(t, s) \quad vs. \quad H_a: C^{(1)}(t, s) \neq C^{(2)}(t, s).$$

Under the H_a , there exists at least one t and s such that the equality is violated. Then we need to find the change-point and divide the whole sequence into two continuous parts at the change-point, and then we can assume a piecewise stationary model for $Y_i(t)$, where the functional covariance is homogeneous in each part.

Under the null hypothesis, we can assume the following model for $\{X_i(t, s): i \in \mathbb{N}\}$,

$$E\{X_i(t, s)\} = C(t, s).$$

We assume $\{X_i(t, s): i \in \mathbb{N}\}$ satisfy the following conditions.

Assumption 1 (A1). $\{X_i(t, s): i \in \mathbb{N}\}$ are symmetric and positive definite kernels, and $E\|X_i(t, s)\|^{2+\delta} < \infty$ for some $\delta \in (0, 1)$.

Assumption 2 (A2). There is a measurable function $f: S^\infty \rightarrow PDL^2(\mathcal{T} \times \mathcal{T})$, where S is a measurable space, and *i.i.d* innovations $\{\epsilon_i: i \in \mathbb{N}\}$ taking values in S , so that under H_0 , $X_i(t, s) = f(\epsilon_i, \epsilon_{i-1}, \dots)$ and under H_a ,

$$X_i(t, s) = \begin{cases} f_1(\epsilon_i, \epsilon_{i-1}, \dots), & i \leq k^* \\ f_2(\epsilon_i, \epsilon_{i-1}, \dots), & i > k^* \end{cases}$$

where f_1, f_2 are defined similarly with f and $PDL^2(\mathcal{T} \times \mathcal{T})$ is the space of square integrable positive definite symmetric kernels defined in $L^2(\mathcal{T} \times \mathcal{T})$.

Assumption 3 (A3). There exists an m -dependent sequence

$$X_{i,m}(t, s) = g(\epsilon_i, \dots, \epsilon_{i-m+1}, \epsilon_{i-m}^*, \epsilon_{i-m-1}^*, \dots),$$

where ϵ_i^* is an independent copy of ϵ_i , such that

$$\sum_{m=0}^{\infty} (E\{\|X_i(t, s) - X_{i,m}(t, s)\|^p\})^{1/p} < \infty.$$

Assumption (A2, A3) can be referred to L^p - m -approximable. The idea of this dependence measure was introduced in Wu (2005), and was extended to functional data in Hörmann & Kokoszka (2015). This assumption quantify the weak dependence of $X_i(t, s)$ and covers most stationary functional time series model. The weak dependence quantified by L^p - m -approximable typically will not influence the consistency property of estimators. As a special case, if a sequence composes of independent functions, it automatically satisfies Assumption (A2, A3).

The current proposed method is developed for single change-point problem, however, we can adapt the procedure to multiple change-point problem, for example, by binary segmentation. However, we do not pursue this problem in the current paper. We now describe our proposed two-stage procedure. In the first stage, we apply the detection procedure to find the most pronounced change-point candidate, and then we apply the testing procedure to test the significance of the candidate. To proceed, we first introduce the following estimators of the functional covariance $C_k^{(1)}$ and $C_k^{(2)}$ for the parts $[1, k]$ and $[k + 1, N]$ to be, respectively,

$$\widehat{C}_k^{(1)}(t, s) = \frac{1}{k} \sum_{i=1}^k X_i(t, s), \quad \widehat{C}_k^{(2)}(t, s) = \frac{1}{N - k} \sum_{i=k+1}^N X_i(t, s).$$

Under the null hypothesis, the difference $\widehat{C}_k^{(1)}(t, s) - \widehat{C}_k^{(2)}(t, s)$ should be relatively close to zero for all $1 < k < N$ and $(t, s) \in \mathcal{T} \times \mathcal{T}$. To reduce the impact of the edges (which have high level of uncertainty due to fewer number of observations), we incorporate a weight function to attenuate the end-point effect. Thus, our proposed weighted difference sequence is

$$\Delta_k(t, s) = \frac{k(N - k)}{N} \left\{ \widehat{C}_k^{(1)}(t, s) - \widehat{C}_k^{(2)}(t, s) \right\} = \sum_{i=1}^k X_i(t, s) - \frac{k}{N} \sum_{i=1}^N X_i(t, s)$$

and large value of $\Delta_k(t, s)$ can be expected for some k, t, s if structural break is present. The detection step is based on the following cumulative statistics (CUSUM)

$$T_N(\theta) = \frac{1}{N} \int \int \left\{ \sum_{i=1}^{[N\theta]} X_i(t, s) - \frac{[N\theta]}{N} \sum_{i=1}^N X_i(t, s) \right\}^2 dt ds,$$

where $k = \lfloor N\theta \rfloor$ and θ is the location of k in the rescaled interval $[0, 1]$. Thus, our proposed test statistic is

$$T_N(\hat{\theta}_N) = \max_{0 \leq \theta \leq 1} T_N(\theta).$$

To determine the change-point candidate, we plot $T_N(\theta)$ against $\theta \in (0, 1)$ and find the argument that maximises $T_N(\theta)$. To ensure uniqueness, we define the change-point candidate as

$$\hat{\theta}_N = \inf\{\theta: T_N(\theta) = \sup_{0 \leq \theta' \leq 1} T_N(\theta')\}.$$

The next step is to apply a formal test to classify the candidate change-point as a change-point or otherwise. The following theorems provides the asymptotic properties of the test statistics under H_0 and H_a .

Theorem 1. Under Assumptions (A1)–(A3) and H_0 ,

$$T_N(\hat{\theta}_N) \xrightarrow{\mathcal{D}} \sup_{\theta \in [0,1]} \sum_{d=1}^{\infty} \rho_d B_d^2(\theta), \quad N \rightarrow \infty.$$

where $(B_d: d \in \mathbb{N})$ are *i.i.d* standard Brownian bridge defined on $[0, 1]$.

Theorem 2. Under Assumption (A1)–(A3) and H_a , $T_N(\hat{\theta}_N) \rightarrow \infty$, $N \rightarrow \infty$.

Remark 1. Theorem 1 validates the asymptotic distribution of the test statistics under H_0 , and provides a threshold, for a given probability of Type I error, for rejecting H_0 .

Remark 2. Note that the asymptotic distribution in Theorem 1 depends on the eigenvalue of $LC_X(t, s, \tilde{t}, \tilde{s})$, which need to be estimated. The procedure of estimating $(\rho_d: d \in \mathbb{N})$ is discussed in Section 3.2.

Remark 3. Theorem 2 tells us the power of the test is asymptotically 1.

3.2 Estimation of ρ_d 's

One key step of the testing procedure is estimating the unknown eigenvalues of the long-run functional covariance $LC_X(t, s, \tilde{t}, \tilde{s})$. As the long-run covariance consists of infinite many lagged functional auto-covariance, we consider the kernel estimator of $LC_X(t, s, \tilde{t}, \tilde{s})$, defined as

$$\widehat{LC}_X(t, s, \tilde{t}, \tilde{s}) = \sum_{h=-\infty}^{\infty} W\left(\frac{h}{\ell}\right) \widehat{C}_{X,h}(t, s, \tilde{t}, \tilde{s}),$$

where $W(\cdot)$ is a symmetric weight function such that, $W(0) = 1$, $W(\cdot) \leq 1$, $W(u) = W(-u)$, $W(u) = 0$ if $|u| > 1$, $W(\cdot)$ is continuous on $[-1, 1]$, and ℓ is the bandwidth parameter that needs to be selected (see e.g. Rice & Shang (2017)). As a special case, when the functions are independent, $W(0) = 1$, and $W(u) = 0, u \neq 0$. Under H_0 , we

can estimate the functional covariance and auto-covariance with the entire sequence as follows,

$$\begin{aligned}\widehat{C}_{X,h}(t, s, \tilde{t}, \tilde{s}) &= \frac{1}{N-h} \sum_{i=1}^{N-h} \{X_i(t, s) - \bar{X}_i(t, s)\} \{X_{i+h}(\tilde{t}, \tilde{s}) - \bar{X}(\tilde{t}, \tilde{s})\}, \quad h \geq 0, \\ \widehat{C}_{X,h}(t, s, \tilde{t}, \tilde{s}) &= \frac{1}{N+h} \sum_{i=1-h}^N \{X_i(t, s) - \bar{X}_i(t, s)\} \{X_{i+h}(\tilde{t}, \tilde{s}) - \bar{X}(\tilde{t}, \tilde{s})\}, \quad h < 0.\end{aligned}$$

Ramsay (2004) described two computational methods for estimating eigenfunctions of two-way functional covariance. The first method is discretizing functional covariances. However, this method cannot be extended to four-way long-run functional covariance. We propose to represent $(X_i(t, s): i \in \mathbb{N})$ by a series of common basis. Given $\{\phi_d(t): d \in \mathbb{N}\}$ being the common basis of $L^2(\mathcal{T})$, $\{\phi_d(t)\phi_{d'}(s): d, d' \in \mathbb{N}\}$ are then the common basis of $L^2(\mathcal{T} \times \mathcal{T})$. If a function $f(t, s)$ is a symmetric function, we have $\langle\langle f(t, s), \phi_d(t)\phi_{d'}(s) \rangle\rangle = \langle\langle f(t, s), \phi_{d'}(t)\phi_d(s) \rangle\rangle$ for any pair of d, d' , therefore we can construct the following basis for two-way symmetric functions,

$$\{\Phi_d(t, s): d \in \mathbb{N}\} = \{\phi_{d_1}(t)\phi_{d_2}(s) + \phi_{d_2}(t)\phi_{d_1}(s): d_1 \neq d_2 \in \mathbb{N}_+\} \cup \{\phi_{d'}(t)\phi_{d'}(s): d' \in \mathbb{N}_+\},$$

Suppose each demeaned function $\widehat{Z}_i(t, s) = X_i(t, s) - \bar{X}(t, s)$ has the following basis approximation,

$$\widehat{Z}_{i,J}(t, s) = \sum_{j=1}^J c_{ij} \Phi_j(t, s). \quad (3-1)$$

where J is selected such that the above J -dimensional approximation is close to the original functions, such that, for some tolerance error of approximation ϵ , J is the smallest dimension that satisfies that the integrated mean squared error of approximation is less than ϵ . Define $C_i = (c_{i,1}, \dots, c_{i,J})$, $\mathbf{C} = (C_1, \dots, C_N)'$, and $\Phi = (\Phi_1, \dots, \Phi_J)'$. We represent the estimator for long-run functional covariance in the following matrix form

$$\widehat{LC}_X(t, s, \tilde{t}, \tilde{s}) = \frac{1}{N} \Phi(t, s)' \mathbf{C}' \mathbf{C} \Phi(\tilde{t}, \tilde{s}).$$

Now suppose that an eigenfunction $\widehat{\psi}(t, s)$ has the following basis expansion

$$\widehat{\psi}(t, s) = \sum_{j=1}^J b_j \Phi_j(t, s) = \Phi(t, s)' \mathbf{b},$$

where $\mathbf{b} = (b_1, \dots, b_J)'$, this yields

$$\begin{aligned}\int \widehat{LC}_X(t, s, \tilde{t}, \tilde{s}) \psi(\tilde{t}, \tilde{s}) d\tilde{t} d\tilde{s} &= \int \frac{1}{N} \Phi(t, s)' \mathbf{C}' \mathbf{C} \Phi(\tilde{t}, \tilde{s}) \Phi(\tilde{t}, \tilde{s})' \mathbf{b} d\tilde{t} d\tilde{s} \\ &= N^{-1} \tilde{\Phi}(t, s)' \mathbf{C}' \mathbf{C} \mathbf{W} \mathbf{b} \\ &= \rho \tilde{\Phi}(t, s)' \mathbf{b},\end{aligned}$$

where W is a $J \times J$ matrix with elements $W_{ij} = \langle\langle \Phi_i, \Phi_j \rangle\rangle$. This equation holds for arbitrary t and s , thus we have

$$N^{-1}W^{1/2}\mathbf{C}'\mathbf{C}W^{1/2}\mathbf{u} = \rho\mathbf{u},$$

where $\mathbf{u} = W^{1/2}\mathbf{b}$. We can solve the eigen-equation to obtain $\{\hat{\rho}_d: d \in \mathbb{N}\}$.

We now summarize the implementation procedure in Algorithm 1,

Algorithm 1 change-point detection and testing

Step 1. For $k = 1, \dots, N$, estimate $C_k^{(1)}, C_k^{(2)}, (\rho_d: d \in \mathbb{N})$, and obtain the test statistics $T_N(\theta)$,

Step 2. Obtain the change-point candidate $\hat{\theta}_N = \min\{\theta: T_N(\theta) = \sup_{\theta': (0,1)} T_N(\theta')\}$,

Step 3. Test the null hypothesis H_0 . If the null hypothesis is rejected, $\hat{\theta}_N$ is declared as a change-point.

3.3 Asymptotic properties of the estimated change-point

We now develop the asymptotic properties of the estimated change-point. Denote $k^* = [N\theta^*]$, where θ^* is fixed and unknown, we will discuss for both scaled ($\hat{\theta}_N^*$) and unscaled change-point (\hat{k}_N^*) estimator under H_a . First we shall show it is consistent in the scaled case, say, $\hat{\theta}_N^* \xrightarrow{p} \theta^*$. For $\theta \in (0, 1)$, we define the following function

$$h(\theta, t, s) = \begin{cases} \theta(1 - \theta^*)(C^{(1)} - C^{(2)}), & 0 < \theta \leq \theta^*, \\ (1 - \theta)\theta^*(C^{(1)} - C^{(2)}), & \theta^* < \theta < 1, \end{cases}$$

where $C^{(1)}$ and $C^{(2)}$ are defined in Equation (3-1). Then we have the following theorem.

Theorem 3. Under the change point model and Assumption (A2), for any t, s , we have

$$T_N(\theta)/N \xrightarrow{p} \int \int h(\theta, t, s) dt ds.$$

Then we can get the consistency of $\hat{\theta}_N^*$ as displayed in the following corollary.

Corollary 1. Under the change-point model and Assumption (A2), we have $\hat{\theta}_N^* \xrightarrow{p} \theta^*$.

This corollary can be easily obtained from Theorem 3. Equivalently, the estimated scaled change-point is the maximizer of $T_N(\theta)/N$. It is evident that the unique maximizer of $\int \int h(\theta, t, s) dt ds$ is θ^* , thus $\hat{\theta}_N^* \xrightarrow{p} \theta^*$.

To discuss the asymptotic distribution of the estimated unscaled change-point, we define

$$U(k) = \begin{cases} \left((1 - \theta^*) \|C^{(2)} - C^{(1)}\|^2 + \frac{1}{|k|} \sum_{i=k^*+k}^{k^*} \langle\langle C^{(2)} - C^{(1)}, X_i - C^{(1)} \rangle\rangle \right) k, & k < 0, \\ \left(-\theta^* \|C^{(2)} - C^{(1)}\|^2 + \frac{1}{k} \sum_{i=k^*}^{k^*+k} \langle\langle C^{(2)} - C^{(1)}, X_i - C^{(2)} \rangle\rangle \right) k, & k \geq 0. \end{cases}$$

The difference between the estimated unscaled change-point \hat{k}_N^* and the true unscaled change-point k^* asymptotically converges to the maximizer of the function $U(k)$ in distribution, which is illustrated in Theorem 4.

Theorem 4. Under Assumption (A1)–(A3), if $C^{(1)} - C^{(2)} \neq 0$, we have

$$\hat{k}_N^* - k^* \xrightarrow{\mathcal{D}} \min \left\{ k : U(k) = \sup_{\tilde{k} \in \mathbb{N}} U(\tilde{k}) \right\}, \quad \text{as } N \rightarrow \infty,$$

Remark 4. The asymptotic distribution of \hat{k}_N^* is influenced by two factors: 1). The discrepancy of covariance structure between the two parts, and 2). The variability of $\{X_i(t, s) : i \in \mathbb{N}\}$ and the alignment between $\{X_i(t, s) - C^{(g)}(t, s) : g = 1, 2, i \in \mathbb{N}\}$ and $C^{(1)}(t, s) - C^{(2)}(t, s)$. As a special case, if $\{X_i(t, s) - C^{(g)}(t, s) : g = 1, 2, i \in \mathbb{N}\}$ are orthogonal to $C^{(1)}(t, s) - C^{(2)}(t, s)$, then the unscaled estimated change-point is always consistent with the true one, in other words, $\hat{k}_N^* \xrightarrow{p} k^*$.

4 Simulations

We simulated two groups of functions with the same sample size and different functional covariances to study the finite sample behaviors of the change-point estimator. The two groups of functions were concatenated as a functional sequence with structural break in the mid-point. For simplicity, we simulated independent functions with mean zero. We selected the 2nd to the 9th Fourier basis over the unit interval $[0, 1]$, denoted by $\nu_1(t), \dots, \nu_8(t)$, to represent the functions. In other words, we simulated functions in δ -frequency band (1-4 Hertz). The independent curves were then generated by

$$Y_i^{(g)}(t) = \sum_{d=1}^8 \xi_{i,d}^{(g)} \nu_d(t) + e_i(t), \quad g = 1, 2,$$

where $\{\xi_{i,d}^{(g)} : d = 1, \dots, 8\}$ are independent normal random variable with standard deviation σ_1 and σ_2 for group 1 and group 2 respectively. Denoting $\mathbf{1}_p$ to be a p -dimensional row vector with all elements to be 1, we consider the following three different forms of standard deviation,

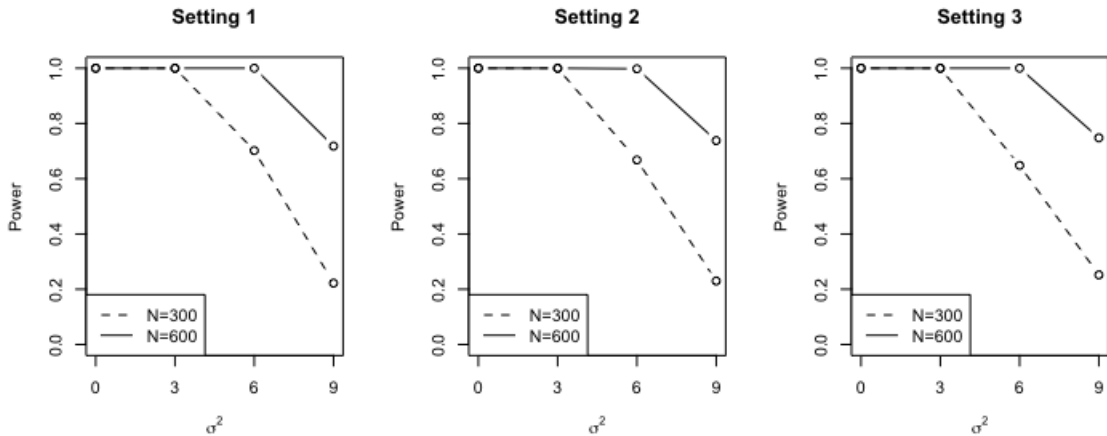
Setting 1: $\sigma_1 = (\mathbf{1}_4, 0.5\mathbf{1}_4)$, $\sigma_2 = (0.5\mathbf{1}_4, \mathbf{1}_4)$;
Setting 2: $\sigma_1 = (\mathbf{1}_2, 0.5\mathbf{1}_2, \mathbf{1}_2, 0.5\mathbf{1}_2)$, $\sigma_2 = (0.5\mathbf{1}_2, \mathbf{1}_2, 0.5\mathbf{1}_2, \mathbf{1}_2)$;
Setting 3: $\sigma_1 = (1, 0.5) \otimes \mathbf{1}_4$, $\sigma_2 = (0.5, 1) \otimes \mathbf{1}_4$.

In the first two settings, the discrepancy between the functional covariances comes from the difference of spectral distribution, and group 1 contains functions that contain mostly low frequency oscillations while functions in group 2 are dominated by high frequencies. In Setting 3, the two groups have the same spectrum but different phase distribution. $\{e_i(t) : i \in \mathbb{N}\}$ are *i.i.d* random error functions satisfying

$$e_i(t) = \sum_{d=1}^8 \xi_{i,d}^{(e)} \nu_d(t),$$

where $\{\xi_{i,d}^{(e)} : d = 1, \dots, 8\}$ are independent normal random variables with mean zero and standard deviation $\sigma_e = \{\sigma/d : d = 1, \dots, 8\}$. We took into account the influence of random error on the detection performance by setting different values to σ , say, $\sigma^2 = 0, 3, 6, 9$. A large value of σ^2 indicates low signal-noise ratio. For each setting, we simulated $N = 150$ or 300 curves for each group and applied our method to find the change-point. The simulation runs were repeated 500 times for different values of σ^2 , and we obtained the cross-validation confidence interval of $\hat{\theta}_N = \hat{k}_N^*/(2N)$. We used the R package “*sde*” to obtain numerical 95% quantile of the null distribution at different θ . Figure 1 displays the power curves for different settings and sample sizes. Table 1 displays the 90% cross validation confidence interval, and Figure 2 displays the Box-plots of $\hat{\theta}_N = \hat{k}_N^*/(2N)$ for different setting and variance parameter σ^2 . We can see that the method works equally well for these three settings with respect to the estimation variability.

Figure 1: Power curves for the three different settings



We would like to stress one interesting point in Setting 3. Two important elements in frequency domain analysis are spectra and phase. When we want to test the structural break in brain signal recordings (i.e. EEG, LPF), we can check the spectrum function

Figure 2: Box-plots of estimated change-point candidate

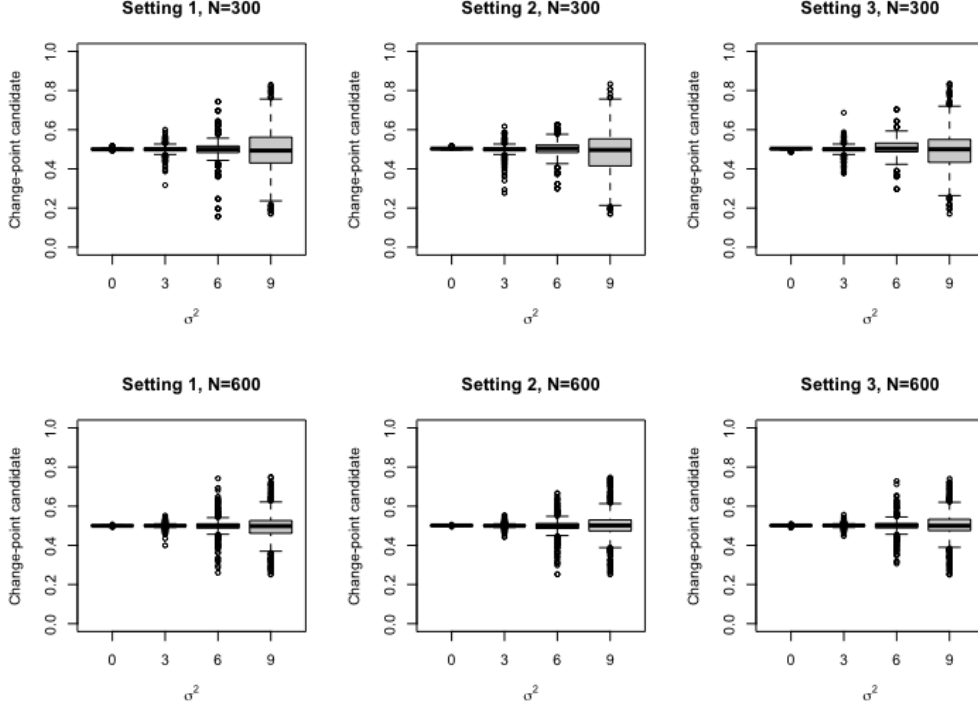


Table 1: Cross-validation 90% confidence interval of change-point candidate $\hat{\theta}_N$

Setting	N	$\sigma^2 = 0$	$\sigma^2 = 3$	$\sigma^2 = 6$	$\sigma^2 = 9$
1	300	(0.497,0.503)	(0.460,0.533)	(0.347,0.617)	(0.286,0.710)
	600	(0.500,0.502)	(0.482,0.513)	(0.428,0.570)	(0.330,0.628)
2	300	(0.500,0.503)	(0.450,0.537)	(0.333,0.627)	(0.266,0.677)
	600	(0.500,0.502)	(0.485,0.518)	(0.408,0.570)	(0.380,0.643)
3	300	(0.500,0.507)	(0.453,0.527)	(0.343,0.633)	(0.296,0.703)
	600	(0.500,0.503)	(0.487,0.515)	(0.422,0.563)	(0.345,0.639)

(see e.g. Schröder and Ombao (2017)), however, under Setting 3, the spectrum function is the same for the entire sequence, and consequently the spectrum-based detection method does not work, but as our functional procedure incorporates intra-curve information, the structural break in phase can also be detected. This is one of the major advantages of our functional procedure.

5 Application on local field potentials

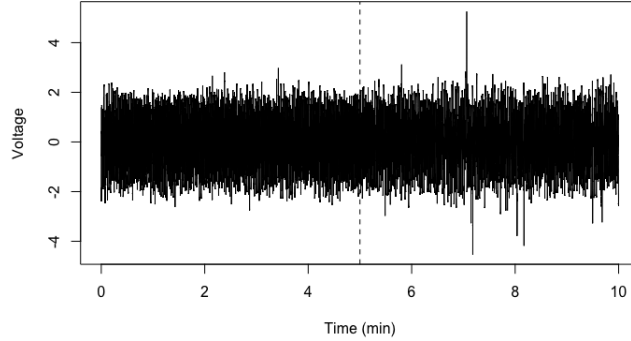
The new method was applied to local field potential (LFP) trajectories of rat brain activity, collected from the experiment of Frostig and Wann (Wann, 2017). Microtetrodes were inserted in 32 locations on the rat cortex. From these microtetrodes, LFPs were

recorded at the rate of 1000 observations per second, and the observations collected in one second is considered as an epoch. The experiment last for 10min and a total of 600 epochs were recorded. Midway in this period (at epoch 300), stroke was mechanically induced on the rat by clamping the medial cerebral artery. As noted, following the stroke, there might be some delay before changes in brain electrophysiological signal taking place. Here we only considered the δ -frequency band (1-4 Hertz), and smooth the trajectory of each epoch with the first 9 Fourier basis specified as follows

$$F_i(t) = \begin{cases} 1, & t \in [0, 1], & \text{if } i = 1, \\ \sqrt{2} \cos(2\pi kt), & t \in [0, 1], & \text{if } i = 2k, \\ \sqrt{2} \sin(2\pi kt), & t \in [0, 1], & \text{if } i = 2k + 1, \end{cases}$$

where $k = 1, 2, 3, 4$. If other frequency bands are of interest, we can represent the trajectories with the Fourier basis in the corresponding frequency band.

Figure 3: The rescaled epochs collected from the first tetrode.

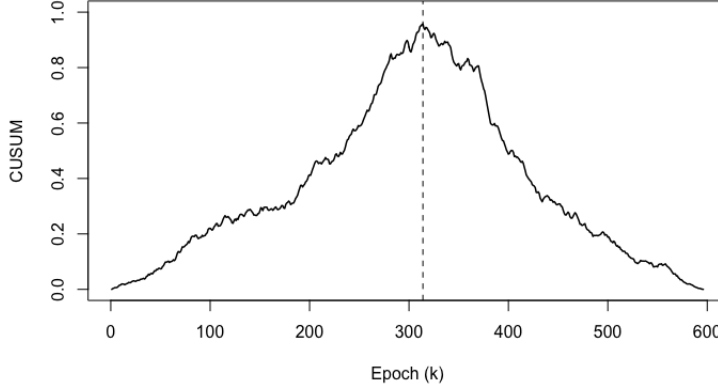


To solve the multiple change-point problem, we applied a binary segmentation procedure. We first considered the entire sequence, and found the most pronounced change-point. Then we divided the sequence into two parts, and applied our method to detect the change-point in each sub-sequence. We repeated the procedure until no more significant change-points were found.

The change-points were detected at epochs 371, 380, 423, 479, and 576. These change-points were tested significant mainly due to the unusual epochs where the signals displayed extremely high variability. However, the change-point candidate near the mid-point was not significant. The reason is that the variability of post-stroke trajectories are not stationary, and the non-stationarity influences the significance of spectral structure discrepancy between the functional covariances of pre and post-stroke trajectories. To remove this effect, we rescaled the trajectories of each epoch to norm one, and applied our procedure to the rescaled trajectories, displayed in Figure 3. The plot of $T_N(\theta)$ is displayed in Figure 4.

After rescaling the trajectories of each epoch, the first change-point candidate is near mid-point (at which is about 14 seconds after stroke), and was test significant at signif-

Figure 4: Values of $T_N(\theta)$ (rescaled epochs).



ificance level $\alpha = 0.05$. The change-point candidate near the mid-point is the only one which was tested significant for rescaled functions. This indicates that the stroke applied on rat cortex caused significant structural break in the spectral structure of functional covariance, and also tells us if we are more interested in the spectral structure than the amplitude, we can work with the functional covariance of rescaled functions.

6 Conclusions

To conclude, we developed a fully functional procedure to identify the change-point in functional covariance. Our proposed method does not require a pre-application of any dimension reduction technique. The procedure is well designed for both independent and correlated functions. The method can be useful when structural breaks are present in the second moment structure (see Jiao et al. (2020)). The scaled estimated change-point is consistent and the two factors influencing the consistency of the estimated unscaled change-point are 1) discrepancy of functional covariance, 2) variability level of random error and the alignment between $\{X_i(t, s) - C^{(g)}(t, s): g = 1, 2, i \in \mathbb{N}\}$ and $C^{(1)}(t, s) - C^{(2)}(t, s)$. Even though this paper focuses on single change-point problem, the procedure can be easily extended to multiple change-point problem by employing approximate detection procedure, such as window sliding, binary segmentation and bottom up segmentation (see e.g. Truong et al. (2020)).

An important application of our method is structural break detection in brain signals. Comparing with other existing methods on this topic, this functional approach has two main advantages. First, it is robust to chance variability since we propose to check the functional covariance of complete epoch trajectories. Additionally, the proposed method incorporates intra-curve information, which is potentially informative of structural break in brain signals. Considering the curse of dimensionality, the methodology requires sample size to be large enough if we want to detect the structural breaks of

the brain signals over a wide frequency band, and dimension reduction techniques will be considered in the future.

References

- ASTON, JOHN AD & KIRCH, CLAUDIA (2012a). Detecting and estimating changes in dependent functional data. *Journal of Multivariate Analysis* **109**, 204–220.
- ASTON, JOHN AD & KIRCH, CLAUDIA (2012b). Evaluating stationarity via change-point alternatives with applications to fMRI data. *The Annals of Applied Statistics* **6**, 1906–1948.
- AUE, ALEXANDER, RICE, GREGORY & SÖNMEZ, OZAN (2020). Structural break analysis for spectrum and trace of covariance operators. *Environmetrics* **31**, e2617.
- AUE, ALEXANDER, RICE, GREGORY & SÖNMEZ, OZAN (2018). Detecting and dating structural breaks in functional data without dimension reduction. *Journal of the Royal Statistical Society: Series B (Statistical Methodology)* **80**, 509–529.
- AUE, ALEXANDER, GABRYS, ROBERTAS, HORVÁTH, LAJOS & KOKOSZKA, PIOTR (2009). Estimation of a change-point in the mean function of functional data. *Journal of Multivariate Analysis* 1043–1073.
- AUE, ALEXANDER, HÖRMANN, SIEGFRIED, HORVÁTH, LAJOS & HUŠKOVÁ, MARIE (2009). Dependent functional linear models with applications to monitoring structural change. *Statistica Sinica* **100**, 2254–2269.
- AUE, ALEXANDER, HÖRMANN, SIEGFRIED, HORVÁTH, LAJOS & REIMHERR, MATTHEW (2009). Break detection in the covariance structure of multivariate time series models. *The Annals of Statistics* **37**, 4046–4089.
- BERKES, ISTVÁN, GABRYS, ROBERTAS, HORVÁTH, LAJOS & KOKOSZKA, PIOTR (2009). Detecting changes in the mean of functional observations. *Journal of the Royal Statistical Society: Series B (Statistical Methodology)* **71**, 927–946.
- BERKES, ISTVÁN, HORVÁTH, LAJOS & RICE, GREGORY (2009). Weak invariance principles for sums of dependent random functions. *Stochastic Processes and their Applications* **123**, 385–403.
- CHO, HAERAN, & Fryzlewicz, Piotr. (2015) Multiple-change-point detection for high dimensional time series via sparsified binary segmentation. *Journal of the Royal Statistical Society: Series B (Statistical Methodology)* **77**, 475–507.
- FERREIRA, JC & MENEGATTO, VA (2009). Eigenvalues of integral operators defined by smooth positive definite kernels. *Integral Equations and Operator Theory* **64**, 61–81.

- FRYZLEWICZ, PIOTR & RAO, S. SUBBA (2014). Multiple-change-point detection for auto-regressive conditional heteroscedastic processes. *Journal of the Royal Statistical Society: Series B (Statistical Methodology)* **76**, 903–924.
- GROMENKO, OLEKSANDR, KOKOSZKA, PIOTR & REIMHERR, MATTHEW (2017). Detection of change in the spatiotemporal mean function. *Journal of the Royal Statistical Society: Series B (Statistical Methodology)* **79**, 29–50.
- HIVELY, LM, PROTOPOPESCU, VA & GAILEY, PC (2000). Timely detection of dynamical change in scalp EEG signals. *Chaos: An Interdisciplinary Journal of Nonlinear Science* **10**, 864–875.
- HÖRMANN, SIEGFRIED & KOKOSZKA, PIOTR (2010). Weakly dependent functional data. *The Annals of Statistics* **38**, 1845–1884.
- JIAO, SHUHAO, RON D. FROSTIG & OMBAO, HERNANDO (2020). Classification of Functional Data by Detecting the Discrepancy of Second Moment Structure of Scaled functions. *arXiv preprint arXiv:2004.00855*
- JONES, RICHARD H, CROWELL, DAVID H & KAPUNIAI, LINDA E (2015). A method for detecting change in a time series applied to newborn EEG. *Electroencephalography and clinical neurophysiology* **27**, 436–440.
- KIRCH, CLAUDIA, MUHSAL, BIRTE & OMBAO, HERNANDO (2015). Detection of changes in multivariate time series with application to EEG data. *Journal of the American Statistical Association* **110**, 1197–1216.
- RAMSAY, J. O. (2004). *Functional data analysis*. Encyclopedia of Statistical Sciences **4**
- RICE, GREGORY & SHANG, HANLIN (2017). A Plug-in Bandwidth Selection Procedure for Long-Run Covariance Estimation with Stationary Functional Time Series. *Journal of time series analysis* **38**, 591–609.
- SCHRÖDER, ANNA LOUISE & OMBAO, HERNANDO (2019). FreSpeD: Frequency-specific change-point detection in epileptic seizure multi-channel EEG data. *Journal of the American Statistical Association* **114**, 115–128.
- SAAID, MF MOHAMED, ABAS, WAB WAN, AROFF, H, MOKHTAR, N, RAMLI, R & IBRAHIM, Z (2011). change-point detection of EEG signals based on particle swarm optimization. *5th Kuala Lumpur International Conference on Biomedical Engineering 2011*, 484–487, Springer.
- SHORACK, GALEN R & WELLNER, JON A (2009). *Empirical processes with applications to statistics*. SIAM.
- SUNDARARAJAN, RAANJU R. & POURAHMADI, MOHSEN (2018). Nonparametric change point detection in multivariate piecewise stationary time series. *Journal of Nonparametric Statistics* **30**, 926–956.

- TORGOVITSKI, LEONID (2015). Detecting changes in Hilbert space data based on” repeated” and change-aligned principal components. *arXiv preprint arXiv:1509.07409*
- TRUONG, CHARLES, OUDRE, LAURENT & VAYATIS, NICOLAS (2017). Selective review of offline change-point detection methods. *Signal Processing* **167**, 107299.
- WANN, ELLEN GENEVIEVE (2017). *Large-scale spatiotemporal neuronal activity dynamics predict cortical viability in a rodent model of ischemic stroke*. Ph.D. dissertation, UC Irvine.
- WU, WEIBIAO (2005). Nonlinear system theory: Another look at dependence. *Proceedings of the National Academy of Sciences* **102**, 14150–14154.

A Proof of Theorem 1 & 2

Under Assumption (A1–A3), we can approximate the weakly dependent process with m -dependent process and study the asymptotic distribution of that approximated m -dependent process. Then we need to show the asymptotic property as m goes to infinity.

It is noted that $T_N(\theta)$ does not change if the $X_i(t, s)$ is replaced with $X_i(t, s) - C(t, s)$. First we show that the result in Theorem 1 can be established for m -dependent random functions. To show the asymptotic result for m -dependent process, we first introduce the following lemma.

Lemma 1. Let

$$S_N(\theta, t, s) = \frac{1}{\sqrt{N}} \sum_{i=1}^{[N\theta]} (X_i(t, s) - C(t, s)).$$

Then, under Assumption (A1)–(A3), there exists a Gaussian process, $(G(\theta, t, s), t, s \in \mathcal{T})$, such that

$$E\{G(\theta, t, s)\} = 0, \quad E\{G(\theta, t, s)G(\tilde{\theta}, \tilde{t}, \tilde{s})\} = \min\{\theta, \tilde{\theta}\}LC_X(t, s, \tilde{t}, \tilde{s}),$$

and

$$\sup_{\theta \in [0,1]} \int \int \{S_N(\theta, t, s) - \Gamma(\theta, t, s)\}^2 dt ds \xrightarrow{p} 0.$$

The proof of Lemma 1 can follow the framework of Berkes et al. (2013). We will not discuss in details but will give a sketch of the proof.

First we need to show that the Lemma holds for a m -dependent process $X_{i,m}(t, s)$, which is constructed as in (A3). We can similarly define the long-run covariance of $X_{i,m}(t, s)$ as follows

$$LC_m(t, s, \tilde{t}, \tilde{s}) = \sum_{i=-m}^m E\{X_{0,m}(t, s)X_{i,m}(\tilde{t}, \tilde{s})\},$$

which is symmetric and positive definite kernel and thus admits the spectral decomposition

$$LC_m(t, s, \tilde{t}, \tilde{s}) = \sum_{d=1}^{\infty} \rho_{m,d} \psi_{m,d}(t, s) \psi_{m,d}(\tilde{t}, \tilde{s}).$$

The series $(\psi_{m,i}(t, s): i \in \mathbb{N})$ forms an sequence of orthonormal basis for $L^2(\mathcal{T} \times \mathcal{T})$, and thus for fixed D and any i ,

$$X_{i,m,D}(t, s) - C_m(t, s) = \sum_{d=1}^D \langle X_{i,m} - C_m, \psi_{m,d} \rangle \psi_{m,d}(t, s),$$

where $C_m(t, s) = E\{X_{i,m}(t, s)\}$. Next we aim to obtain the asymptotic property of

$$\frac{1}{\sqrt{N}} \sum_{i=1}^{[N\theta]} X_{i,m,D}(t, s) - C_m(t, s),$$

and it is equivalent to study the D dimensional random process

$$\left(\frac{1}{\sqrt{N}} \sum_{i=1}^{[N\theta]} \langle X_{i,m} - C_m, \psi_{m,1} \rangle, \dots, \frac{1}{\sqrt{N}} \sum_{i=1}^{[N\theta]} \langle X_{i,m} - C_m, \psi_{m,D} \rangle \right), \quad (1-1)$$

then by Lemma 2 in the following, we can show quantity 1-1 converge in distribution to

$$\left(\rho_{m,1}^{1/2} W_{m,1}(\theta), \dots, \rho_{m,D}^{1/2} W_{m,D}(\theta) \right),$$

where $(W_{m,i}(\theta): i = 1, \dots, D)$ are *i.i.d* Wiener processes.

Lemma 2. If (A1)–(A3), then the D dimensional random process (1-1), as $N \rightarrow \infty$, converges to

$$\left(\rho_{m,1}^{1/2} W_{m,1}(\theta), \dots, \rho_{m,D}^{1/2} W_{m,D}(\theta) \right).$$

proof of Lemma 2. First we specify the covariance of the asymptotic distribution of (1-1). For $d_1 \neq d_2$,

$$\begin{aligned} & E \left\{ \frac{1}{\sqrt{N}} \sum_{i=1}^{[N\theta]} \langle X_{i,m} - C_m, \psi_{m,d_1} \rangle, \frac{1}{\sqrt{N}} \sum_{j=1}^{[N\theta]} \langle X_{j,m} - C_m, \psi_{m,d_2} \rangle \right\} \\ &= \frac{[N\theta]}{N} \frac{1}{[N\theta]} \sum_{i,j=1}^{[N\theta]} E \{ \langle X_{i,m} - C_m, \psi_{m,d_1} \rangle \langle X_{j,m} - C_m, \psi_{m,d_2} \rangle \} \\ &\rightarrow \theta \langle LC_m(\psi_{m,d_1}), \psi_{m,d_2} \rangle = 0 \end{aligned}$$

By central limit theorem for m -dependent random variables, for each d , we have

$$\begin{aligned} \frac{1}{\sqrt{N}} \sum_{i=1}^{[N\theta]} \langle X_{i,m} - C_m, \psi_{m,d} \rangle &= \sqrt{\frac{[N\theta]}{N}} \frac{1}{\sqrt{[N\theta]}} \sum_{i=1}^{[N\theta]} \langle X_{i,m} - C_m, \psi_{m,d} \rangle \\ &\xrightarrow{\mathcal{D}} \theta \mathcal{N}(0, \rho_{m,d}). \end{aligned}$$

Thus the lemma follows. \square

Consequently, since $X_i(t, s)$ is uniformly square integrable by (A1), we have

$$\sup_{\theta \in [0,1]} \int \int \left(\frac{1}{\sqrt{N}} \sum_{i=1}^{[N\theta]} (X_{i,m,D}(t, s) - C_m(t, s)) - \sum_{d=1}^D \rho_{m,d}^{1/2} W_{m,d}(\theta) \phi_{m,d}(t, s) \right)^2 dt ds \xrightarrow{p} 0$$

Then we need to show that the reminder $X_{i,m} - X_{i,m,D}$ is trivial asymptotically. Evidently,

$$\lim_{D \rightarrow \infty} \sup_{\theta \in [0,1]} \int \int \left(\frac{1}{\sqrt{N}} \sum_{i=1}^{[N\theta]} X_{i,m,D}(t, s) - \frac{1}{\sqrt{N}} \sum_{i=1}^{[N\theta]} X_{i,m}(t, s) \right)^2 dt ds \xrightarrow{p} 0,$$

$$\lim_{D \rightarrow \infty} \sup_{\theta \in [0,1]} \int \int \left(\sum_{d=D+1}^{\infty} \rho_{m,d}^{1/2} W_{m,d}(\theta) \phi_{m,d}(t, s) \right)^2 dt ds \xrightarrow{p} 0$$

and this leads to

$$\lim_{D \rightarrow \infty} \sup_{\theta \in [0,1]} \int \int \left(\frac{1}{\sqrt{N}} \sum_{i=1}^{[N\theta]} (X_{i,m}(t, s) - C_m(t, s)) - \sum_{d=1}^D \rho_{m,d}^{1/2} W_{m,d}(\theta) \phi_{m,d}(t, s) \right)^2 dt ds \xrightarrow{p} 0.$$

Define $R_m(\theta, t, s) = \sum_{d=1}^{\infty} \rho_{m,d}^{1/2} W_{m,d}(\theta) \psi_{m,d}(t, s)$, and we now check the property of $R_m(\theta, t, s)$. By basis expansion,

$$R_m(\theta, t, s) = \sum_{d=1}^{\infty} \langle R_m(\theta), \psi_d \rangle \psi_d(t, s),$$

The joint distribution of $\langle R_m(\theta), \psi_d \rangle$, $d \in \mathbb{N}$ is normal with zero mean. Hence they converge jointly to a multivariate normal distribution for any $m \in \mathbb{N}_+$. To specify the joint asymptotic distribution, we only need to find the covariance. As $m \rightarrow \infty$,

$$\begin{aligned} E \langle R_m(\theta_1), \psi_d \rangle \langle R_m(\theta_2), \psi_{d'} \rangle &= \min(\theta_1, \theta_2) \langle C_m(\psi_d), \psi_{d'} \rangle \\ &\rightarrow \min(\theta_1, \theta_2) \langle C(\psi_d), \psi_{d'} \rangle \\ &= \min(\theta_1, \theta_2) \rho_d \mathbb{I}\{d = d'\}. \end{aligned}$$

By Skorokhod-Dudley-Wichura theorem (Shorack et al. (2009)), there exists independent Wiener processes $(W_d(\theta) : d = 1, \dots, D)$, such that for any θ , so as $N \rightarrow \infty$,

$$\lim_{D \rightarrow \infty} \sup_{\theta \in [0,1]} \int \int \left(\frac{1}{\sqrt{N}} \sum_{i=1}^{[N\theta]} (X_i(t, s) - C(t, s)) - \sum_{d=1}^D \rho_d^{1/2} W_d(\theta) \phi_d(t, s) \right)^2 dt ds \xrightarrow{p} 0.$$

Furthermore, since as $D \rightarrow \infty$,

$$\sup_{\theta \in [0,1]} \int \int \left(\sum_{d=D+1}^{\infty} \rho_d^{1/2} W_d(\theta) \phi_d(t, s) \right)^2 dt ds \leq \sum_{d=D+1}^{\infty} \rho_d \rightarrow 0,$$

we can conclude

$$\sup_{\theta \in [0,1]} \int \int \left(\frac{1}{\sqrt{N}} \sum_{i=1}^{[N\theta]} (X_i(t, s) - C(t, s)) - \sum_{d=1}^{\infty} \rho_d^{1/2} W_d(\theta) \phi_d(t, s) \right)^2 dt ds \xrightarrow{p} 0.$$

Then we can finish the proof of Lemma 1.

Proof of Theorem 1. First, as $N \rightarrow \infty$, it is evident that the influence of

$$X_i(t, s), \min([N\theta], N\theta) \leq i \leq \max([N\theta], N\theta)$$

is trivial on T_n , in other words,

$$T_n = \sup_{0 \leq \theta \leq 1} \|S_N(\theta, t, s) - \theta S_N(1, t, s)\|^2 + o_p(1).$$

Next we need to show

$$\sup_{0 \leq \theta \leq 1} \|S_N(\theta, t, s) - \theta S_N(1, t, s)\|^2 \xrightarrow{p} \sup_{0 \leq \theta \leq 1} \|G(\theta, t, s) - \theta G(1, t, s)\|^2$$

By triangular inequality and Lemma 1, we have

$$\begin{aligned} & \sup_{0 \leq \theta \leq 1} \|S_N(\theta, t, s) - \theta S_N(1, t, s)\|^2 - \sup_{0 \leq \theta \leq 1} \|G(\theta, t, s) - \theta G(1, t, s)\|^2 \\ & \leq \sup_{0 \leq \theta \leq 1} \{ \|S_N(\theta, t, s) - \theta S_N(1, t, s)\|^2 - \|G(\theta, t, s) - \theta G(1, t, s)\|^2 \} \\ & = O_p(1) \sup_{0 \leq \theta \leq 1} \{ \|S_N(\theta, t, s) - \theta S_N(1, t, s)\| - \|G(\theta, t, s) - \theta G(1, t, s)\| \} \\ & \leq O_p(1) \sup_{0 \leq \theta \leq 1} \{ \|S_N(\theta, t, s) - \theta S_N(1, t, s) - (G(\theta, t, s) - \theta G(1, t, s))\| \} \\ & = o_p(1). \end{aligned}$$

As $G(\theta, t, s)$ is a Gaussian process, by simple verification of its first two moments, $G(\theta, t, s) - \theta G(1, t, s)$ should follow the same distribution as $\sum_{d=1}^{\infty} \sqrt{\rho_d} B_d(\theta) \psi_d(t, s)$, where $(B_d: d \in \mathbb{N})$ are standard Brownian bridge on $\mathcal{T} \times \mathcal{T}$. Consequently,

$$\sup_{0 \leq \theta \leq 1} \|G(\theta, t, s) - \theta G(1, t, s)\|^2 \stackrel{\mathcal{D}}{=} \sup_{\theta \in [0, 1]} \sum_{d=1}^{\infty} \rho_d B_d^2(\theta).$$

The proof is then complete. \square

Proof of Theorem 2. First we define the following quantity for the following argument

$$S_{N, k^*, Z} = \frac{1}{\sqrt{N}} \left(\sum_{i=1}^{k^*} Z_i(t, s) - \frac{k^*}{N} \sum_{i=1}^N Z_i(t, s) \right),$$

where $Z_i = X_i - C^{(g)}$, $g = 1, 2$. By definition, we have $T_N(\hat{\theta}_N) \geq T_N(\theta^*)$. Then we have that

$$\begin{aligned} T_N(\hat{\theta}_N) & \geq \left\| \frac{1}{\sqrt{N}} \left(\sum_{i=1}^{k^*} X_i - \frac{k^*}{N} \left\{ \sum_{i=1}^{k^*} X_i + \sum_{i=k^*+1}^N X_i \right\} \right) \right\|^2 \\ & = \left\| S_{N, k^*, Z} - \frac{k^*}{\sqrt{N}} \frac{N - k^*}{N} (C^{(2)} - C^{(1)}) \right\|^2 \\ & \geq \left\| \frac{k^*}{\sqrt{N}} \frac{N - k^*}{N} (C^{(2)} - C^{(1)}) \right\|^2 - \|S_{N, k^*, Z}^0(\theta^*)\|^2 \\ & = \left\| \sqrt{N} \theta^* (1 - \theta^*) (C^{(2)} - C^{(1)}) \right\|^2 - \|S_{N, k^*, Z}^0(\theta^*)\|^2. \end{aligned}$$

By Lemma 1, $\|S_{N, k^*, Z}^0(\theta^*)\| = O_p(1)$, therefore, $T_N \rightarrow \infty$ as $N \rightarrow \infty$. Then the theorem is proved. \square

B Proof of Theorem 3 & 4

Proof of Theorem 3. We first show $\Delta_k(t, s)/N \xrightarrow{p} h(\theta, t, s)$, when $\theta \in (0, \theta^*]$, by ergodic theorem,

$$\begin{aligned}\Delta_k(t, s)/N &= \frac{1}{N} \sum_{i=1}^k X_i - \frac{k}{N^2} \left(\sum_{i=1}^{k^*} X_i + \sum_{i=k^*+1}^N X_i \right) \\ &\xrightarrow{p} \theta C^{(1)} - \theta (\theta^* C^{(1)} + (1 - \theta^*) C^{(2)}) \\ &= \theta(1 - \theta^*)(C^{(1)} - C^{(2)}),\end{aligned}$$

and when $\theta \in (\theta^*, 1)$,

$$\begin{aligned}\Delta_k(t, s)/N &= \frac{1}{N} \left(\sum_{i=1}^{k^*} X_i + \sum_{i=k^*+1}^k X_i \right) - \frac{k}{N^2} \left(\sum_{i=1}^{k^*} X_i + \sum_{i=k^*+1}^N X_i \right) \\ &\xrightarrow{p} \theta^* C^{(1)} + (\theta - \theta^*) C^{(2)} - \theta \theta^* C^{(1)} - \theta(1 - \theta^*) C^{(2)} \\ &= (1 - \theta) \theta^* (C^{(1)} - C^{(2)}),\end{aligned}$$

Then by $T_N(\theta)/N = \int \int \Delta_k(t, s)/N dt ds$, the proof is finished. \square

The proof of Theorem 4 requires the following two lemmas.

Lemma 3. Under Assumption (A1)–(A3), $|\hat{k}_N^* - k^*|$ is bounded in probability.

Proof of Lemma 3. Obviously we have

$$\hat{k}^* = \min\{k: R_{N,k} = \max_{1 \leq k' \leq N} R_{N,k'}\},$$

where $R_{N,k} = 1/N(\|\Delta_k\|^2 - \|\Delta_{k^*}\|^2)$. When $k < k^* - L$,

$$\begin{aligned}R_{N,k} &= \frac{1}{N} \int \int \left(\sum_{i=1}^k X_i - \frac{k}{N} \sum_{i=1}^N X_i \right)^2 - \left(\sum_{i=1}^{k^*} X_i - \frac{k^*}{N} \sum_{i=1}^N X_i \right)^2 dt ds \\ &= \frac{1}{N} \langle D_k^{(1)} + E_k^{(1)}, D_k^{(2)} + E_k^{(2)} \rangle,\end{aligned}$$

where

$$E_k^{(1)} = - \sum_{i=k+1}^{k^*} Z_i + \frac{k^* - k}{N} \left(\sum_{i=1}^{k^*} Z_i + \sum_{i=k^*+1}^N Z_i \right), \quad D_k^{(1)} = \frac{(k^* - k)(N - k^*)}{N} (C^{(2)} - C^{(1)}),$$

$$E_k^{(2)} = \sum_{i=1}^k Z_i + \sum_{i=1}^{k^*} Z_i - \frac{k^* + k}{N} \left(\sum_{i=1}^{k^*} Z_i + \sum_{i=k^*+1}^N Z_i \right), \quad D_k^{(2)} = - \frac{(k^* + k)(N - k^*)}{N} (C^{(2)} - C^{(1)}),$$

and $Z_i = X_i - C^{(g)}$. For $k \in [1, k^* - L]$, we will show that $\langle\langle D_k^{(1)}, D_k^{(2)} \rangle\rangle$ is the dominant term,

$$\begin{aligned} \left| \langle\langle D_k^{(1)}, D_k^{(2)} \rangle\rangle \right| &= \frac{(k^* - k)(k + k^*)(N - k^*)^2}{N^2} \|C^{(1)} - C^{(2)}\|^2 \\ &\geq \frac{(k^* - k)k^*(N - k^*)^2}{N^2} \|C^{(1)} - C^{(2)}\|^2 \\ &= \|C^{(1)} - C^{(2)}\|^2 \theta^* (1 - \theta^*)^2 N (k^* - k) \end{aligned}$$

Letting $c = \|C^{(1)} - C^{(2)}\|^2 \theta^* (1 - \theta^*)^2$, by Cauchy-Schwarz inequality,

$$\begin{aligned} \max_{1 \leq k \leq k^* - L} \frac{\left| \langle\langle E_k^{(1)}, E_k^{(2)} \rangle\rangle \right|}{\left| \langle\langle D_k^{(1)}, D_k^{(2)} \rangle\rangle \right|} &\leq \max_{1 \leq k \leq k^* - L} \frac{\|E_k^{(1)}\| \|E_k^{(2)}\|}{c N (k^* - k)}, \\ &\leq \frac{1}{c} \max_{1 \leq k \leq k^* - L} \frac{\|E_k^{(1)}\|}{k^* - k} \max_{1 \leq k \leq k^* - L} \frac{\|E_k^{(2)}\|}{N} \end{aligned}$$

also we have

$$\begin{aligned} \max_{1 \leq k \leq k^* - L} \frac{\|E_k^{(1)}\|}{k^* - k} &= \max_{1 \leq k \leq k^* - L} \left\| -\frac{1}{k^* - k} \sum_{i=k+1}^{k^*} Z_i + \frac{1}{N} \left(\sum_{i=1}^{k^*} Z_i + \sum_{i=k^*+1}^N Z_i \right) \right\| \\ &\leq \max_{1 \leq k \leq k^* - L} \left(\frac{1}{k^* - k} \left\| \sum_{i=k+1}^{k^*} Z_i \right\| + \left\| \frac{1}{N} \left(\sum_{i=1}^{k^*} Z_i + \sum_{i=k^*+1}^N Z_i \right) \right\| \right) \\ &= \max_{1 \leq k \leq k^* - L} \left(\frac{1}{k^* - k} \left\| \sum_{i=k+1}^{k^*} Z_i \right\| \right) + \left\| \frac{\theta^*}{k^*} \sum_{i=1}^{k^*} Z_i + \frac{1 - \theta^*}{N - k^*} \sum_{i=k^*+1}^N Z_i \right\|, \end{aligned}$$

where the first term is $o_p(1)$ by Lemma B.1 in Aue et al. (2018), and the second term is $o_p(1)$ by ergodic theorem in $L^2(\mathcal{T} \times \mathcal{T})$. By ergodic theorem, for any $k \in [1, k^* - L]$,

$$\max_{1 \leq k \leq k^* - L} \frac{\|E_k^{(2)}\|}{N} \leq \max_{1 \leq k \leq k^* - L} \left(\frac{1}{N} \left\| \sum_{i=1}^k Z_i \right\| + \frac{1}{N} \left\| \sum_{i=1}^{k^*} Z_i \right\| + \frac{k + k^*}{N^2} \left\| \sum_{i=1}^N Z_i \right\| \right) = o_p(1).$$

Also we can conclude that

$$\max_{1 \leq k \leq k^* - L} \frac{\left| \langle\langle E_k^{(1)}, D_k^{(2)} \rangle\rangle \right|}{\left| \langle\langle D_k^{(1)}, D_k^{(2)} \rangle\rangle \right|} \xrightarrow{p} 0, \quad \max_{1 \leq k \leq k^* - L} \frac{\left| \langle\langle D_k^{(1)}, E_k^{(2)} \rangle\rangle \right|}{\left| \langle\langle D_k^{(1)}, D_k^{(2)} \rangle\rangle \right|} \xrightarrow{p} 0$$

Then for any $\epsilon < 0$, we have

$$\lim_{L \rightarrow \infty} \limsup_{N \rightarrow \infty} P \left(\max_{1 \leq k \leq k^* - L} R_{n,k} > \epsilon \right) = 0.$$

Similarly, we have

$$\lim_{L \rightarrow \infty} \limsup_{N \rightarrow \infty} P \left(\max_{k^* + L \leq k \leq N} R_{n,k} > \epsilon \right) = 0.$$

Since \hat{k}^* is equivalent with the maximum argument of $R_{N,k}$, and R_{N,k^*} . Thus

$$P\left(|\hat{k}^* - k^*| > L\right) \leq P\left(\max_{1 \leq k \leq k^* - L} R_{n,k} > \epsilon\right) + P\left(\max_{k^* + L \leq k \leq N} R_{n,k} > \epsilon\right),$$

and consequently,

$$\lim_{L \rightarrow \infty} \limsup_{N \rightarrow \infty} P\left(|\hat{k}_N^* - k^*| > L\right) = 0.$$

□

Lemma 4. With Assumption (A1)–(A3), then

$$(R_{N,k^*+k} : k \in [-L, L]) \xrightarrow{\mathcal{D}} (2\theta(1-\theta)U(k) : k \in [-L, L]), \quad N \rightarrow \infty$$

for any $L \geq 1$.

Proof of Lemma 4. As $k \in [k^* - L, k^*]$,

$$\begin{aligned} \frac{1}{N} \langle\langle D_k^{(1)}, D_k^{(2)} \rangle\rangle &= (k - k^*) \left(\frac{k + k^*}{N} \right) \left(\frac{N - k^*}{N} \right)^2 \|C^{(1)} - C^{(2)}\|^2 \\ &\rightarrow 2(k - k^*)\theta(1 - \theta)^2 \|C^{(1)} - C^{(2)}\|^2. \end{aligned}$$

$$\begin{aligned} \frac{1}{N} \langle\langle D_k^{(2)}, E_k^{(1)} \rangle\rangle &= \frac{(N - k^*)(k + k^*)(k - k^*)}{N^3} \sum_{i=1}^N \langle\langle Z_i, C^{(2)} - C^{(1)} \rangle\rangle \\ &\quad + \frac{(N - k^*)(k + k^*)}{N^2} \sum_{i=k+1}^{k^*} \langle\langle Z_i, C^{(2)} - C^{(1)} \rangle\rangle \\ &\rightarrow 2\theta(1 - \theta) \sum_{i=k+1}^{k^*} \langle\langle Z_i, C^{(2)} - C^{(1)} \rangle\rangle, \end{aligned}$$

as the first term converges to zero in probability by ergodic theorem. Then we need to show the term $\langle\langle E_k^{(1)}, E_k^{(2)} \rangle\rangle/N$ and $\langle\langle D_k^{(1)}, E_k^{(2)} \rangle\rangle/N$ is negligible in the asymptotic distribution. By Cauchy-Schwarz inequality,

$$\frac{1}{N} \left| \langle\langle E_k^{(1)}, E_k^{(2)} \rangle\rangle \right| \leq \|E_k^{(1)}\| \left\| \frac{1}{N} E_k^{(1)} \right\|, \quad \frac{1}{N} \left| \langle\langle D_k^{(1)}, E_k^{(2)} \rangle\rangle \right| \leq \|D_k^{(1)}\| \left\| \frac{1}{N} E_k^{(2)} \right\|$$

By triangular inequality and ergodic theorem,

$$\begin{aligned} \|E_k^{(1)}\| &\leq \left\| \sum_{i=k+1}^{k^*} Z_i \right\| + L \left\| \frac{1}{N} \sum_{i=1}^N Z_i \right\| \\ &\leq \left\| \sum_{i=k+1}^{k^*} Z_i \right\| + L \left\| \frac{k^*}{N} \left(\frac{1}{k^*} \sum_{i=1}^{k^*} Z_i \right) + \frac{N - k^*}{N} \left(\frac{1}{N - k^*} \sum_{i=1}^{N - k^*} Z_i \right) \right\| \\ &= O_p(1) + o_p(1), \end{aligned}$$

and by ergodic theorem,

$$\frac{1}{N} \|E_k^{(2)}\| \leq \frac{1}{N} \left\| \sum_{i=1}^k Z_i \right\| + \frac{1}{N} \left\| \sum_{i=1}^{k^*} Z_i \right\| + \frac{k+k^*}{N^2} \left\| \sum_{i=1}^N Z_i \right\| = o_p(1).$$

Therefore

$$\frac{1}{N} \left| \langle\langle E_k^{(1)}, E_k^{(2)} \rangle\rangle \right| = o_p(1),$$

and similarly, we have

$$\frac{1}{N} \left| \langle\langle D_k^{(1)}, E_k^{(2)} \rangle\rangle \right| = o_p(1).$$

As $k^* - L \leq k \leq k^*$, this leads to

$$R_{N,k} \xrightarrow{p} 2(k^* - k)\theta(1 - \theta)^2 \|C^{(1)} - C^{(2)}\|^2 + 2\theta(1 - \theta) \sum_{i=k+1}^{k^*} \langle\langle Z_i, C^{(1)} - C^{(2)} \rangle\rangle,$$

and similarly, as $k^* < k < k^* + L$,

$$R_{N,k} \xrightarrow{p} -2(k - k^*)\theta^2(1 - \theta) \|C^{(1)} - C^{(2)}\|^2 + 2\theta(1 - \theta) \sum_{i=k^*+1}^{k^*+k} \langle\langle Z_i, C^{(1)} - C^{(2)} \rangle\rangle,$$

□

Combining the result of Lemma 3 and Lemma 4, we can obtain Theorem 3. Lemma 3 indicates we can study the asymptotic property on a bounded interval $[\hat{k}^* - L, \hat{k}^* + L]$, and then we can obtain the asymptotic result on $[\hat{k}^* - L, \hat{k}^* + L]$, and letting $L \rightarrow \infty$, by continuous mapping theorem, we can prove Theorem 4.